SHADRACK, BOADU AFRANE. M.S. Mechanical Evaluation of Various Geometrical Designs in Additive Manufacturing for Future Knee Brace Harness. (2024.)
Directed by Dr. Dennis Lajeunesse. 53 pp.

Additive manufacturing, commonly known as 3D printing, has gained significant inclination due to its numerous benefits in processing and manufacturing. Among all human joints, the knee joint is the most involved in day-to-day activities and is highly susceptible to injuries. Therefore, a well-designed knee brace with enhanced mechanical and geometric properties holds the potential to offer effective diverse support to the knee joint in the future. This project explored the use of additive manufacturing and computer-aided design, specifically OpenSCAD, to design and print six (3) different geometric shapes (simple grid, offset grid, and grid with diamond holes) with five (5) different photopolymer resins (thermochromic resin, water washable resin, standard translucent photopolymer resin, standard plant-based photopolymer resin and ABS-like resin).

The ultimate tensile strength of each print and young's modulus were also analyzed using the stable micro system analyzer. Analysis revealed the simple grid has the best tensile strength with a stress value (4.136 N/mm^2) and (YM~2.299MPa) whilst the geometry with the least tensile strength was the offset grid with a tensile strength value of (0.217 N/mm^2) and YM~0.111MPa). Other mechanical properties such break strain and elastic behavior were also analyzed. Thermochromic and standard photopolymer resin exhibited the highest ultimate tensile strength. This depicts the effects of varying geometries and resin types on the mechanical properties of materials which provides a valuable insight for future development in the field of customizable knee brace fabrication.

MECHANICAL EVALUATION OF VARIOUS GEOMETRICAL DESIGNS IN ADDITIVE MANUFACTURING FOR FUTURE KNEE BRACE HARNESS

By

Shadrack Boadu Afrane

A Thesis
Submitted to
The Faculty of The Graduate School at
The University of North Carolina at Greensboro,
in Partial Fulfillment
of the requirement for the Degree
Master of Science

Greensboro

2024

Approved by

_____

Dr. Dennis LaJeunesse
Committee Chair

APPROVAL PAGE

This thesis written by Shadrack Boadu Afrane has been approved by the following committee of the Faculty of The Graduate School at The University of North Carolina at Greensboro.

Committee Chair

Dr. Dennis Lajeunesse

Committee Members

Dr. Daniel Herr

Dr. Eric Josephs

April 23, 2024

Date of Acceptance by Committee

April 23, 2024

Date of Final Oral Examination

ACKNOWLDEGEMNTS

I would like to express my sincere gratitude to my supervisor, Dr. Dennis R. Lajeunesse, for believing in my abilities, guiding, and supporting me through the entire research process. His expertise and invaluable feedback have been instrumental in shaping this research. I extend my heartfelt appreciation to my lab members, Paul Modey, Adnan Karim, and Dr. Hunter Holding, for their constructive criticism, training, and diverse perspectives, which contributed significantly to the success of this research.

To my committee members, Dr. Daniel Herr, Dr. Eric Josephs, and Dr. Dennis R. Lajeunesse, I extend a heartfelt thank you for your time and willingness to be part of my success story by providing insightful feedback and comments.

I would also like to acknowledge UNC Greensboro and JSNN for providing the facilities and resources that made my dream a reality.

Lastly, I am indebted to my family members and friends for their love, support, words of encouragement, and prayers, which kept me going throughout this project.

TABLE OF CONTENTS

LIST OF TABLES

LIST OF FIGURES

CHAPTER I: INTRODUCTION.

1.1 Background and literature.

3D printing also known as additive manufacturing is the construction of three-dimensional object from a computer aided design in layers. This technology which was first introduced as a stereolithography in 1986 has gained attention in the society by transforming the concept of engineering advanced materials(Li et al., 2020). The advantages of 3D printing over conventional manufacturing techniques are the assurance of precision, flexibility, accuracy, speed, and control. It is also a powerful tool in creating almost all complex objects or geometry. Rapid Prototyping is the end results of additive printing which enhance fabrication of prototypes quickly.

There are quite a few established rapid prototyping techniques that are being utilized. These types include stereolithography (SLA), Powder bed fusion, fused deposition modeling (FDM), laminated object manufacturing (LOM), inkjet printing and contour grafting techniques (Rengier et al., 2010). Because of the ability of this technology to manufacture a diverse range of medical implants through CT-scan images of tissue, it has garnered interest in the medical community(Stansbury & Idacavage, 2016). In the field of construction, WinSun successfully applied 3D printing to mass print adorable houses in China priced at $4800 USD per unit in 24hours(Wu et al., 2016). The technique type used in this project is stereolithography.

1.2 Types of 3D printing.

1.2.1 Stereolithography

SLA technology uses a computer-controlled UV-laser beam for photopolymerization. This laser beam helps to turn a liquid material into a solid one, layer by layer, creating a 3D object. It builds object by adding tiny bits at a time. This method allows for making objects very precisely and with a smooth surface(Lakkala et al., 2023). The laser beam is the energy source that aid in the photopolymerization process to achieve a strong interconnected polymer from monomers (Zakeri et al., 2020). SLA technique uses a liquid polymer called resin to print a pre-programmed shape from a computer-aided design. Resins are UV-active and convert to polymer instantly when activated. Resins are generally categorized into, standard resin, engineering resins, dental and medical resins, castable resins and biomaterial resins. This project focused on utilizing five distinct types of Elegoo Mars 3 compatible resins namely, thermochromic resin, water washable resin, standard translucent photopolymer resin, standard plant-based photopolymer resin and ABS-like resin.

Stereolithography set up is of three components, a container that holds photocurable resins, a source of UV light which initiates polymerization and cross linking of liquid resins, and a system that permit movement of laser beams in the X, Y AND Z direction. Liquid resins solidify by absorbing photons when they are exposed to an ultra-violet light in specific two-dimensional shape. This hardening goes deeper than the thickness of each layer being built(Lakkala et al., 2023). After the initial process, where not all reactive components have fully transformed, additional steps are necessary. These steps involve removing any leftover resin by washing and then subjecting the material to UV light to improve its mechanical properties. SLA has extraordinary resolution as low as 10micrometer and print exceptional quality parts which

can be beneficial in complex structure printing (Wang et al., 2017).Some challenges associated with SLA are slow printing, cost, and limited range of material for printing.

1.2.2 Powder bed fusion.

Powder bed fusion processes involve stacking and fusing thin layers of fine powders onto a platform to construct a 3D part. Layers are tightly packed and fused together using a laser or binder, with subsequent layers added on top until completion. There is an elimination of excess powder by vacuuming. For precision and additional refinement, additional steps such as coating, sintering and infiltration is performed. The density and effectiveness of the printed part is affected by distribution and packaging of the powder(Gibson et al., 2015). Powder bed fusion excels in providing fine resolution and high-quality printing, making it highly suitable for printing intrinsic structures. Advanced applications such as scaffolds for tissue engineering, lattices, aerospace, and electronics make use of powder bed fusion. It is however characterized as slow printing, expensive and porous prone when binders are used to fuse the powder.

1.2.3 Fused deposition modelling (FDM).

This is another technique of 3D printing that involves printing successive layer of materials using continuous filament of thermoplastic polymer. To convert the filament to a partial liquid state, there is a heating that occurs at the nozzle which is then extruded on top of a previously printed layer. The filament has a thermoplastic feature which facilitates fusing and solidification at room temperature. The mechanical properties can be influenced by various processing parameters, including layer thickness, width, and orientation(Ngo et al., 2018). FDM offers key benefits such as affordability, rapid production, and ease of use. It however has drawbacks which includes weak mechanical properties, visible layering, and poor surface quality (Chohan et al., 2017).

1.2.4 Laminated Object Manufacturing (LOM).

LOM is among the commercialized pioneers of 3D printing methods that creates objects in a layer by layer cutting and lamination of sheets. A laser or mechanical cutter is used to sharpen subsequent layers precisely and then joined together. Surplus materials after cutting provides support during the printing process which can be taken away and reused after the process is done(Gibson et al., 2015). Ultrasonic Additive Manufacturing (UAM), a type of laminated object manufacturing, stands out as the sole additive manufacturing method capable of constructing metal structures at low temperatures(Hahnlen & Dapino, 2014). Industries such as paper manufacturing, foundry industries, electronics and smart structures have all used LOM. LOM is ideal for larger structures but not complex shapes because it offers decreased tooling expenses and shorter production times. However, compared to bed-powder method, it has reduced exactness, surface quality and sometimes arduous taking out surplus materials after printing(Ngo et al., 2018)

1.2.5 Inkjet printing and contour grafting technique.

This is another well-known AM technique for printing ceramics. In this process, a mixture of ceramic powder, like zirconium oxide, and water is pushed through a nozzle onto a surface. The material forms a pattern of droplets that harden enough to support additional layers(Dou et al., 2011). It is applied in the field of tissue engineering for printing complex scaffolds. For printing intricate structure, the inkjet method is proven to be effective and quick. Wax-based and liquid suspension are the two main types of ceramic inks. Wax-based ink is melted and hardened when poured on cold surface while liquid suspension solidifies as their liquid component evaporate.

Factors that affect the quality of inkjet printer structures are as follows, thickness, particle distribution size of ceramics, viscosity of the ink and the amount of content, size of the nozzle and the speed of printing (Travitzky et al., 2014). Contour grafting which is almost identical to inkjet printing is utilized in AM of large building structures. It uses giant nozzles and high pressure to push out concrete paste or soil. Interestingly this method is being prototyped for construction on the moon (Khoshnevis, 2004).

1.3 Applications of AM

This remarkable technology, known as additive manufacturing (AM), has found widespread utility across diverse fields including aerospace, biomedical, construction, electronics, and more. The following sections delve into some specific areas where this technology has been applied.

1.3.1 Biomedical.

In the biomedical field such as research and clinical setting, additive manufacturing has gain enormous attention and application because it has the capability to design and print virtual geometrical shapes using materials such as metals, polymers, ceramics and bioinks. Due to the unique features of additive manufacturing, in contrast to conventional methods which are costly, time-consuming, and limited in their ability to produce complex designs and geometries, additive manufacturing is expected to continue gaining popularity and play a significant role in healthcare(Zadpoor, 2017). Some applications in the biomedical fields are:

Tissue engineering: This involves the design and fabrication of biological substitutes that can restore, maintain, or improve tissue function. Additive manufacturing allows researchers and scientists to produce three-dimensional models that closely resemble the complex network of connective tissues found in the human body at a microscopic scale(Ahangar et al., 2019).

Example of such application is implants. Implants and prothesis are constantly gaining advancement to allow for comfort, compatibility and improve functioning among users. 3D printing has connected the field of biology and engineering seamlessly with improved collaboration because of its ability to create sophisticated structures with unique material properties that promote tissue regeneration and integration within the body(Ahangar et al., 2019).

In the field of orthopedics, additive manufacturing, computer-aided design, and radiological imaging techniques are utilized to design and fabricate custom-fit implants tailored to meet the needs of patients with severe and challenging deformities.(Haglin et al., 2016). The significant qualities of 3D printing materials, including porosity, bioabsorbability, osteoinductiveness, and feasibility, render it an ideal tool in orthopedics.

Drug delivery. 3D printing plays distinctive responsibility in the pharmaceutical industries(Gioumouxouzis et al., 2019). Researchers continue to explore various advanced routes and techniques for drug administration, as it remains an area of ongoing interest and investigation. A couple of new ways where 3D printing is being applicable to improve drug delivery are;

Tablets: tablets are solid form drugs that are manufactured by compressing a powder mixture that contains active pharmaceutical ingredients into molds(Ahangar et al., 2019). Although this process is efficient in producing large number of simple tablets, the introduction of additive manufacturing aids in producing customized, unique, and complex tablets for varying patients. "In a study by Khaled et al. (2015), FDM and a hydroalcoholic gel-based paste were used to print a three-compartment tablet capable of releasing three different therapeutics (captopril, nifedipine, glipizide)" (Khaled et al., 141). Their finding was intriguing because while

one drug, Captopril, was released at a constant rate (zero-order kinetics), the release of the other two drugs followed different kinetics, such as first-order kinetics.

Transdermal delivery: This approach involves delivering drugs through the skin's circulation, serving as a distribution network, without the need for invasive methods. Examples of this approach includes patches and micro needling. Stereolithography, a method within additive manufacturing, is utilized to create microneedles with exceptional precision and efficiency, enabling rapid fabrication(Pere et al., 2018).

Surgical Tools: Due to diverse surgical procedures and anatomical variations among patient, customized tools created with additive manufacturing help to provide control and stability during operative experiences, ultimately leading to reduced risks and complications (Liu et al., 2017).

1.3.2 Aerospace.

A report from Wohler indicates a hopeful future for the aerospace industry, with additive manufacturing (AM) encompassing 18.2% of the total market (Wohler, 2017). AM offers unique advantages for aerospace applications, including the ability to print complex geometries, challenging-to-machine materials, and achieving a high buy-to-fly ratio. Additionally, AM allows for easily customizable parts production and high-performance-to-weight ratios. In the aerospace sector, AM can be utilized for producing or repairing components such as turbine blades, aero engine components, heat exchangers, and interiors (Yin et al., 2018).

1.3.3 Building.

Another report from Wohler indicates the architectural industry only comprise 3% of the total market of AM (Wohler, 2017). This is because AM gained attention in the building industry for residential structure just recently in 2014 but has henceforth shown amazing potential since

its introduction. AM can bring a revolutionary improvement in the construction industry as well as making life easier for astronauts(Labeaga-Martínez et al., 2017). In the construction sector, 3D printing finds application in areas facing challenges like complex geometries and hollow structures. Its dependability stems from its precision fabrication capability, which in turn enables a wide range of design options. Khoshnevis pioneered contour crafting (CC) technology for automated building and infrastructure construction, including applications in space(Khoshnevis, 2004).

1.4 Materials (polymers and composites).

Polymers are widely recognized and extensively utilized materials in 3D printing due to their versatility and suitability for most additive manufacturing (AM) processes. They are available in various forms such as resins, filaments, reactive monomers, and powders. Extensive research has been conducted over the years on the industrial applications of polymers and composites in diverse fields including aerospace, toy manufacturing, architecture, and medicine. Composite 3D printing offers several advantages over traditional methods such as molding and extrusion, including the ability to print complex geometries in less time and at a lower cost (Ngo et al., 2018). Photopolymer resin in stereolithography (SLA) printing is activated using ultraviolet light as the energy source.

1.5 Mechanical properties and tensile strength testing.

Mechanical properties of AM structures are essential for products to be able to withstand high pressure from testing. Due to the nonlinear tensile stress-strain response characteristics associated with soft tissues such as muscles, tendons, and ligaments, it poses a challenge to manufacture a device that can mechanically reproduce soft tissue, especially when these tissues become tight(Pattinson et al., 2019). The mechanical properties of tissue types vary considerably

and exhibit different characteristics in different directions. This variability not only depends on the type of tissue but also varies between individuals based on their body type and overall health (Śmietański et al.,2012). Factors such as proper process planning activities like choosing proper parameters, inclusion of additives, post-curing timing period affect mechanical properties of AM prototypes.

Findings from experiments conducted by Chockalingam et al (2006) suggest that various parameters, including layer thickness, post-curing time, and build orientation, play crucial roles in determining the tensile strength of printed objects in additive manufacturing. ‘’Yang et al (2018) experimentally explored the anisotropies of stiffness and strength of 3D printed polymers using the SLA process and performed further structural designs using topology optimization aiming to enhance the mechanical behaviors’’.

Guideline from ASTM standard for testing tensile strength of plastics advice that tensile properties play a critical role in plastics engineering design, providing valuable data for material characterization. However, the sensitivity of many plastics to factors such as strain rate and environmental conditions necessitates caution in the interpretation of test results. Data obtained from standard tensile tests may not accurately represent real-world applications involving different load-time scales or environments. Therefore, it is essential to conduct comprehensive testing across a range of load-time scales and environmental conditions, including impact and creep, to ensure the reliability and applicability of tensile properties in engineering design. As per an article featured on astm.org, the tensile properties assessment of resin-matrix composites reinforced with continuous or discontinuous high modulus fibers exceeding 20 GPa (equivalent to >3.0 x 106 psi) should adhere to the D3039/D3039M Test Method.

1.6 problem statement.

The advantages of 3D printing in contrast to conventional manufacturing techniques encompass the assurance of precision, flexibility, accuracy, speed, and control. Furthermore, it serves as a potent tool for fabricating a wide array of complex objects or geometries. Despite the utility of conventional manufacturing methods, particularly in the fabrication of support braces over the years, they still pose limitations in knitting and weaving concerning mechanical abilities.

An application of AM was demonstrated in a study conducted by Pattinson and colleagues, wherein additive manufacturing techniques were employed to fabricate biomechanically customized meshes for wearable ankle and hand braces (Pattinson et al, 2019). They demonstrated how explicit programming of the toolpath in an extrusion AM process can enable new, flexible mesh materials having digitally tailored mechanical properties and geometry. However, their research focused solely on a specific geometry, and they did not investigate how different geometries might affect the mechanical properties of the materials.

Additionally, their study did not explore the use of different printing materials or polymers, preventing them from determining if the choice of polymer influenced the resulting geometry. To address these limitations, this research aims to investigate different geometries and photopolymer resin types to know which geometry presents the best mechanical property for mass production. Also, to investigate biomechanical properties of additively manufacture meshes for knee brace.

1.7 Specific objectives.

I. To determine the mechanical properties of different geometries in knee sleeves

II. To determine the mechanical properties of different photopolymer resins with varying geometries

III. To determine 3D prints with a good tensile property suitable for large scale production.

CHAPTER II: METHODOLOGY AND MATERIALS

2.1 Study site.

The study was conducted in the Genomic lab at the Joint School of Nanoscience and Nanoengineering. This is a multidisciplinary lab that is equipped with state-of-the- arts equipment rendering it conducive for conducting successful projects. Prior to commencing the research, training sessions were conducted to ensure safety protocols and equipment operation, facilitating the smooth execution of the study.

2.1.2 Study design.

A cross sectional study design was used to analyze the mechanical properties of different geometrical designs.

2.2 Equipment and Materials.

These materials and equipment were used for the study, Elegoo mars 3 3D printer, elegoo mars 3 compatible resins, Elegoo wash and cure station, texture analyser, and a computer aided design (Openscad,chitubox).

2.2.1 Elegoo Mars 3 3D Printer

Elegoo is a company that is known for providing affordable and high-quality resin 3D printers. Among their diverse range of 3D printers, the one utilized for this research within the genomic lab is the Elegoo Mars 3 3D series, Launched in 2022. This is a user-friendly printer released as the first ultra-precision 3D printer with an LCD display that allows seamless operation. The equipment is equipped with a 6.6-inch ultra 4K monochrome LCD display and a 2.0 printing film which provide high precision, visuals, adhesion, and stability of printed layers. The printing technology employed in this equipment is Stereolithography, and it uses UV light with a wavelength of 405nm to enable the photopolymerization process, where liquid resin is solidified

layer by layer to create complex 3D objects. It has a print time ranging between 1.5 to 3 seconds which offers efficient and rapid production capabilities.

The ELEGOO Mars 3 is equipped with the capability to print materials with a remarkably small layer thickness of just 0.01mm. This feature played a pivotal role in its selection for this research project. A notable difference between this machine and conventional 2K LCD 3D printers is its larger printing volume, which surpasses that of the Mars 2 by 37%. Additionally, it boasts an XY precision of up to 35 microns, representing a 30% increase compared to the Mars 2. Furthermore, it demonstrates higher printing efficiency while demanding less maintenance. The equipment includes an air purifier with a built-in active carbon filter, designed to efficiently absorb and filter resin odors and strong fumes, ensuring a fresh and pleasant printing environment.

Figure 2. 1 an image of Elegoo Mars 3 3D printer.

2.2.2 Wash and cure station.

This station serves as a post-processing station for the removal of surplus resin from printed objects, followed known as the Elegoo Mercury XS bundle. The initial component is designed for the washing phase and is equipped with a reservoir containing Isopropanol or alcohol. This solution effectively cleanses the printed objects by eliminating any excess uncured resins, thereby ensuring thorough cleaning prior to the curing process.

The other component of the station features an UV-LED light source, essential for initiating the curing process. This light emits a wavelength that activates the resins within the printed objects, facilitating the curing process. It also includes a rotating platform mechanism, ensuring uniform exposure of the objects to the UV light from all angles. This process facilitates the drying and solidification of the resin within a specific timeframe. The image below shows a picture of the wash and cure station.

Figure 2. 2 The wash and cure station

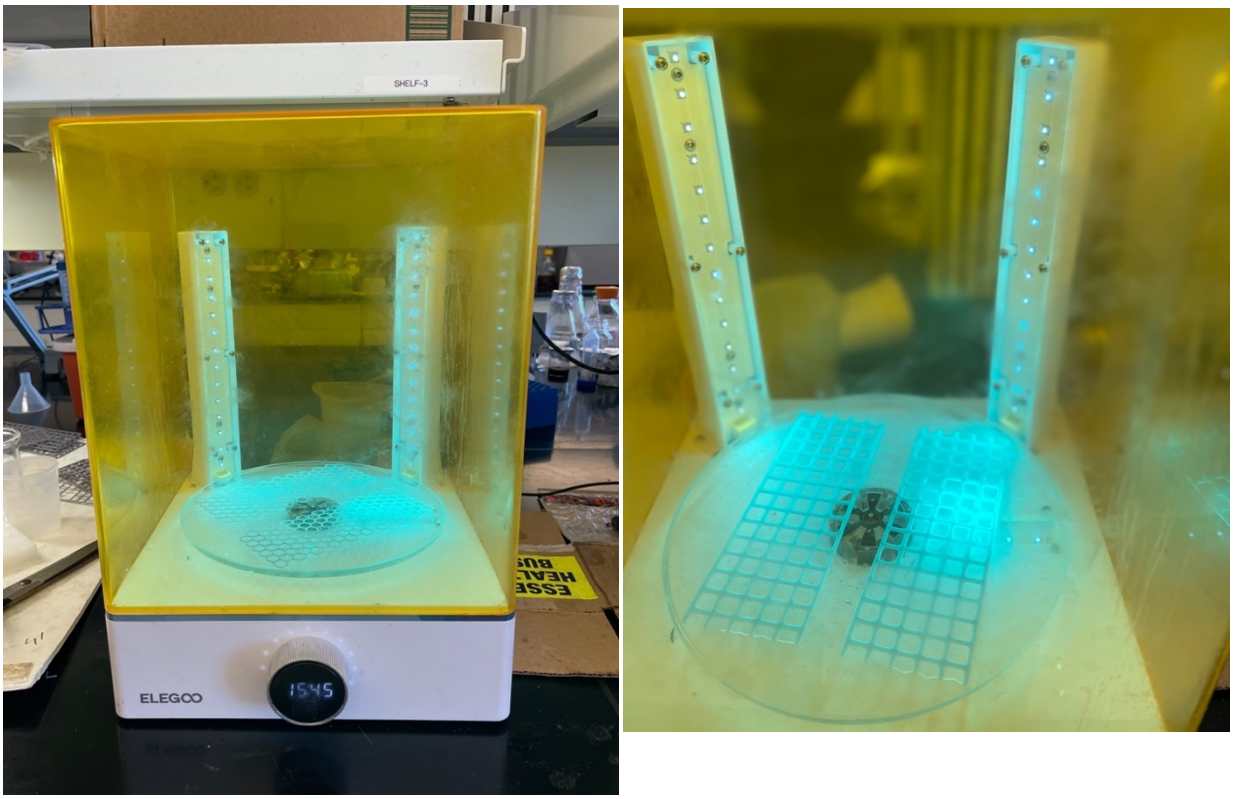

2.2.3 Photopolymer Resins

Resins exhibit UV reactivity and undergo rapid polymerization upon activation. They are commonly classified into several categories, including standard, engineering, dental, medical, castable, and biomaterial resins. This project specifically centered on the utilization of five unique types of Elegoo Mars 3 compatible resins. These resins comprise thermochromic, water washable(grey), standard translucent photopolymer, standard plant-based photopolymer (grey), and ABS-like resins (light blue). Five different types of resins were selected for diversity and comparison since each resin has different parameters for printing. These parameters are listed below.

1. Thermochromic Resin

At a temperature of 50 degrees celcius this resin changes colour from grey to purple.

Parameter settings for slicing into chitubox:

Exposure time= 7s

Bottom exposure time = 45s

Lift distance (mm) = 5

Layer height (mm) = 0.05

Lift speed (mm/min) = 110

Retract speed (mm/min) = 280

2. Water washable(grey)

Parameter settings for slicing into chitubox:

All sample designs were printed perfectly with no difficulties.

Exposure time= 6s

Bottom exposure time = 60s

Lift distance (mm) = 5

Layer height (mm) = 0.05

Lift speed (mm/min) = 110

Retract speed (mm/min) = 280

3. Standard translucent photopolymer.

Parameter settings for slicing into chitubox:

Exposure time= 3s

Bottom exposure time = 45s

Lift distance (mm) = 5

Layer height (mm) = 0.05

Lift speed (mm/min) = 110

Retract speed (mm/min) = 280

4. Standard plant-based photopolymer (grey)

Parameter settings for slicing into chitubox:

Exposure time= 5s

Bottom exposure time = 70s

Lift distance (mm) = 5

Layer height (mm) = 0.05

Lift speed (mm/min) = 110

Retract speed (mm/min) = 280

5. ABS-like resins (light blue)

Parameter settings for slicing into chitubox

Exposure time= 2.5s

Bottom exposure time = 35s

Lift distance (mm) = 5

Layer height (mm) = 0.05

Lift speed (mm/min) = 80Retract speed (mm/min) = 210

2.2.4 Computer aided design.

This is the use of computer software to create, modify or optimize a design. It enables the creating of a 2D or 3D complex structures. This study utilized an OpensCad version 2021.01 to design all prototypes in a 3D format. OpensCAD is a free software that is used for creating solid 3D objects. It has series of programming commands for geometry and operation that allows for control over the design process.

Chitubox version 1.9.0 which is a slicing software was also used to prepare the 3D files for printing by slicing them into thin layers for the printer to understand and print.

2.2.5 Texture analyser.

The Stable Micro System analyzer was utilized to evaluate the tensile strength of all printed materials in this study. With precise force and displacement sensors, this instrument enabled accurate testing of tensile strength. It is also capable of conducting compression force tests and analyzing textile profiles. Renowned for its user-friendly interface, it does well in assessing the mechanical properties of diverse materials.

Figure 2. 3 The Stable Micro System analyzer

2.3 Designing of prototypes.

Three different geometries that would allow for higher order designs to be fabricated were utilized for this project.

Design 1, known as the simple grid, was designed to show what the most basic geometry would enable. In doing so, we set a canvas to base our measurements off. The idea of a grid is nothing new with similarities to woven fabrics and netting.

Design 2, known as the offset simple grid, uses design one as a starting point, but with the grid set 45 degrees to the overall insert. With this rotation of the grid, the mechanical stressors are set at the most extreme angle to the simple grid, this enables the ability to model differing angles of alignment and was believed to improve the stretch of the insert.

Design 3, known as the grid with diamond holes, is a combination of the designs 1,2, and 3. In doing so we developed a higher order geometry while increasing the understanding of the hole doping impact on the mechanical properties of the material.

The sample prototypes were initially sketched, following which their designs were crafted using OpensCAD software in a 3D. The subsequent section outlines the geometries and dimensions utilized in this research. The dimensions used were X-150, Y-50mm, Z-1mm.

Figure 2. 4 sketch of geometries from Openscad software.

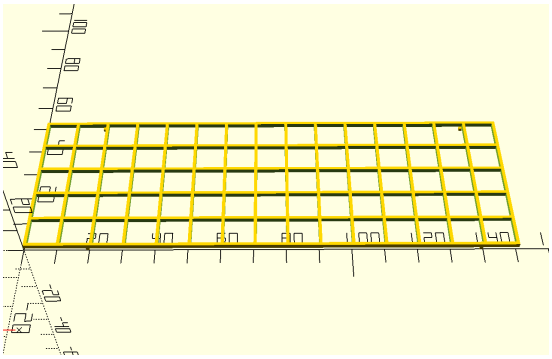

1. Simple grid

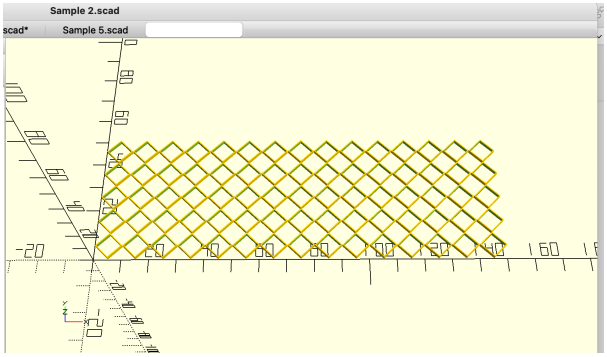

2. Offset Simple Grid

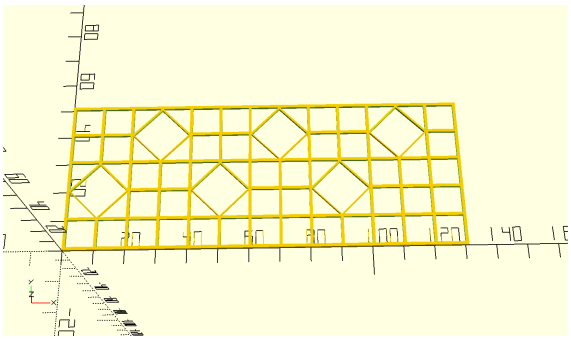

3.Grid with diamond holes.

2.4 Printing and testing process

I printed 65 materials with three specific geometric designs namely (simple grid, grid with diamond hole and offset grid); and the steps I used are stated below.

- Printing of materials began after the proposed geometries in 3D utilizing the openSCAD software version 2021.01.
- Files were then converted to STL format and sliced using chitubox version 1.9.0 to ensure compatibility with the printer.
- The prototypes were transferred onto a pendrive and subsequently loaded into the Elegoo Mars 3 3D printer to initiate the printing process.
- The duration of each print was recorded for every geometry type and resin variant.
- Upon completion of the printing process, the prints underwent a washing procedure in an alcohol container to remove any excess material, followed by removal from the Elegoo Mars 3 3D printer platform using a scraper.
- Subsequently, the prints were exposed to UV light for 20 minutes to enhance drying and optimize mechanical properties.
- The materials underwent testing utilizing a texture analyzer known as the Stable Micro System.
- Prints were inserted into the machine, and parameters were configured to record the tensile strength of each print.
- This sequence of steps was replicated for all 65 printed samples.

2.5 Data Analysis and representation.

Data collected was organized and analyzed in Microsoft Excel version 16.83 and MySQL Workbench version 8.0.33. MySQL was used to write queries to extract data into various tables and analysis and was performed in MS Excel.

CHAPTER III: RESULTS AND ANALYSIS

3.1 Print times

In this study I printed a total of 65 materials with 5 different photopolymer resin in 3 different geometrical shapes.

An observation revealed that prints produced using the ABS-like (blue) resin and the translucent photopolymer resin had reduced thickness, whereas prints from the remaining resins displayed optimal thickness.

Moreover, prints from standard plant-based photopolymer (grey) resin, thermochromic resins and water washable(grey) were more brittle as compared to the ABS-like(blue) and the translucent photopolymer resin.

Additionally, it was noted that the offset simple grid prototype consistently adhered more firmly to the printer platform, resulting in difficulties during removal, potential breakages, and occasionally incomplete print outcomes. This led to an inability to print materials for offset simple grid design using ABS like and Translucent photopolymer resins after several attempt.

Although same dimension was used on the X, Y and Z axis for the design of all prototypes in the openSCAD software it was observed that, due to variations in printing parameters for different resin types, there were variabilities in print times for different resins with different geometries. Thermochromic resin had a prolong print duration as compared to ABS-like and translucent photopolymer resin with comparatively shorter print times.

Table 3. 1 below shows the time It took to print various geometry under various resins.

Resin type	Geometry	Print time (mins)	Average Print time (mins)
Standard Photopolymer Resin (Plant based)	Simple grid	6.14	
	Offset Simple Grid	5.12	
	Grid with diamond holes	8.3	6.52
Translucent photopolymer resin	Simple grid	7.12	
	Offset Simple Grid		
	Grid with diamond holes	5	6.06
Water-washable (grey)	Simple grid	10	
	Offset Simple Grid	9.25	
	Grid with diamond holes	8.12	9.12
ABS-like Resin (Blue)	Simple grid	6	
	Offset Simple Grid		
	Grid with diamond holes	5	5.50
Thermochromic resin	Simple grid	11	
	Offset Simple Grid	12	

	Grid with diamond holes	9	10.66

3.2 Printed meshes.

The figures below show the some of the various designs and how they came out. Texture differences were noticed in the various prototypes based on the type of resin used. The Translucent and ABS-like resins produced the prototypes with reduction in thickness as compared to the other three (3) Resins.

Figure 3. 1 Images of some printed meshes compared from different resin types: A. Translucent photopolymer resin print, B. Standard grey resin C. Water – washable resin(grey).

A 

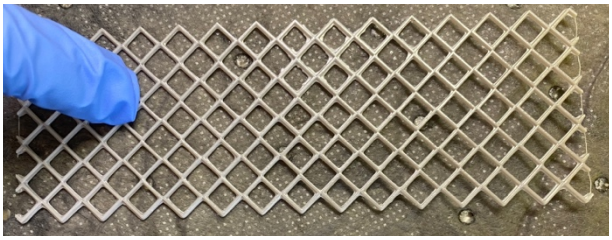

B

C 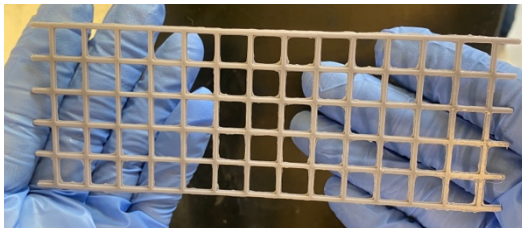

3.3 Mechanical strength analysis.

After the mechanical properties were enhanced for each prototype, mechanical properties analysis was performed. Data was collected, organized and stress-strain curves were plotted from the averages of the individual values obtained for 3 prototypes tested. The following results were obtained for the various resin types and prototypes.

3.3.1 Stress-Strain Curve

The tensile stress-strain curve was plotted from the average of individual values from three tested prototypes. The highest peak of Stress in N/mm^2 represents a good tensile property.

(I) Standard Photopolymer Resin.

The simple grid design demonstrated the best tensile property by having a peak stress value of 4.136 N/mm^2 whilst the geometry with the least tensile strength was the offset grid with a stress value of 1.425 N/mm^2.

Figure 3.2. 1 Stress-strain plot: Simple grid.

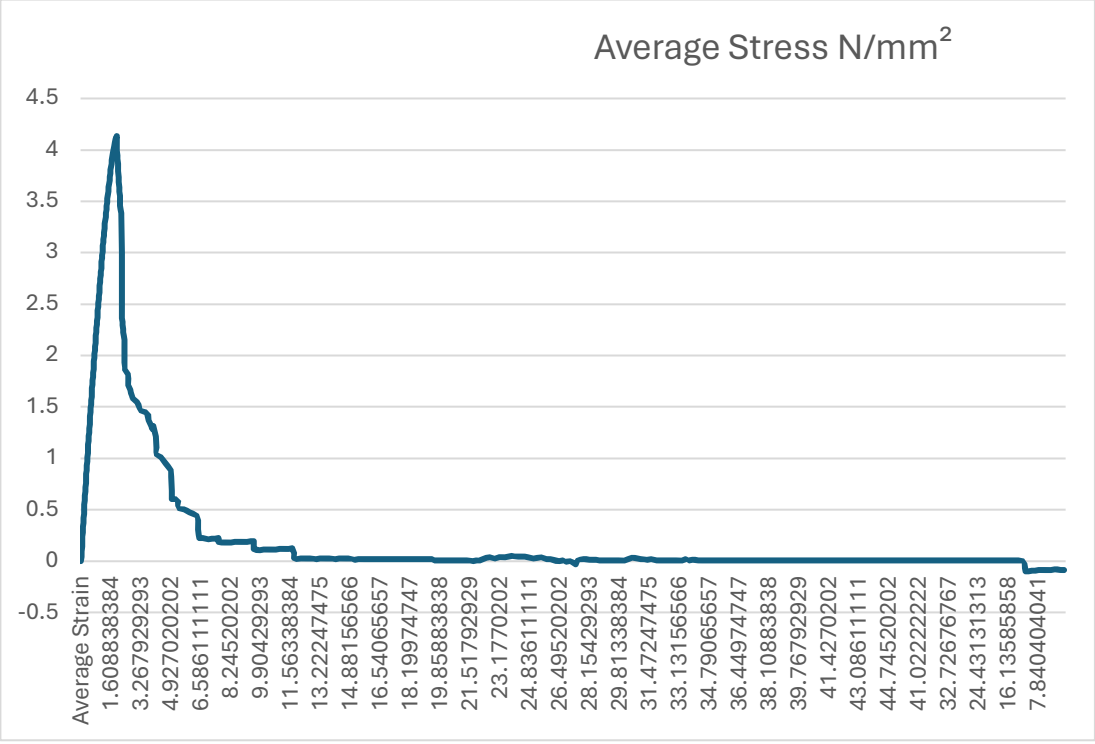

Figure 3.2. 2 Stress-strain plot: Offset Simple grid.

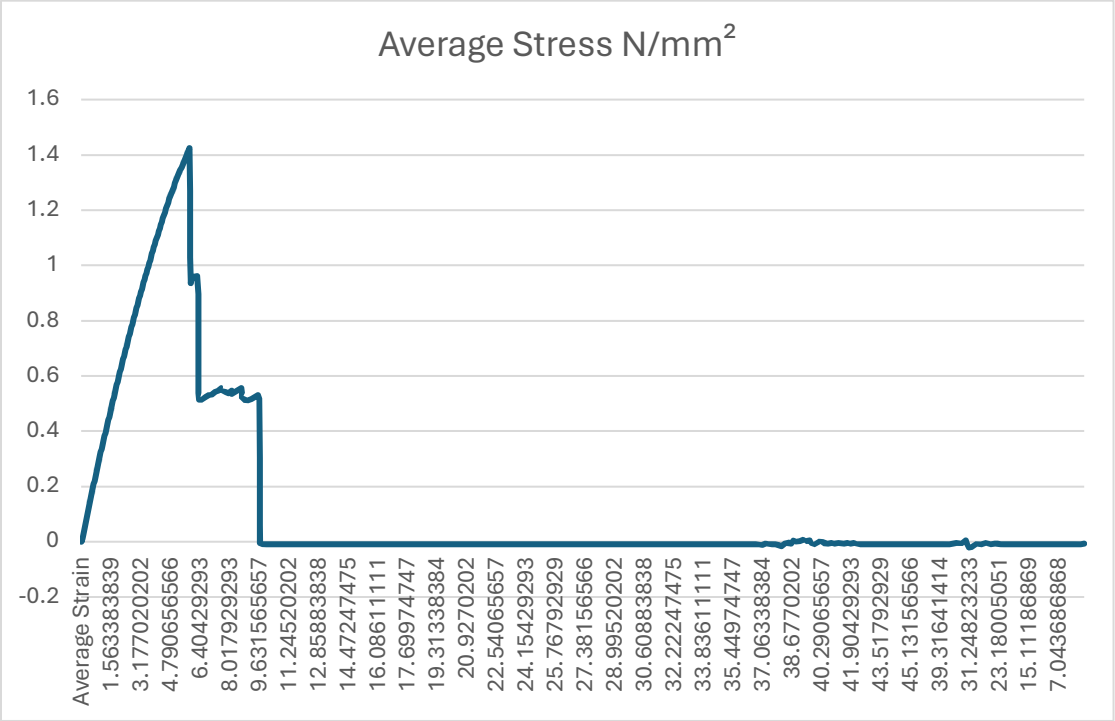

Figure 3.2. 3 Stress-strain plot: Grid with diamond holes

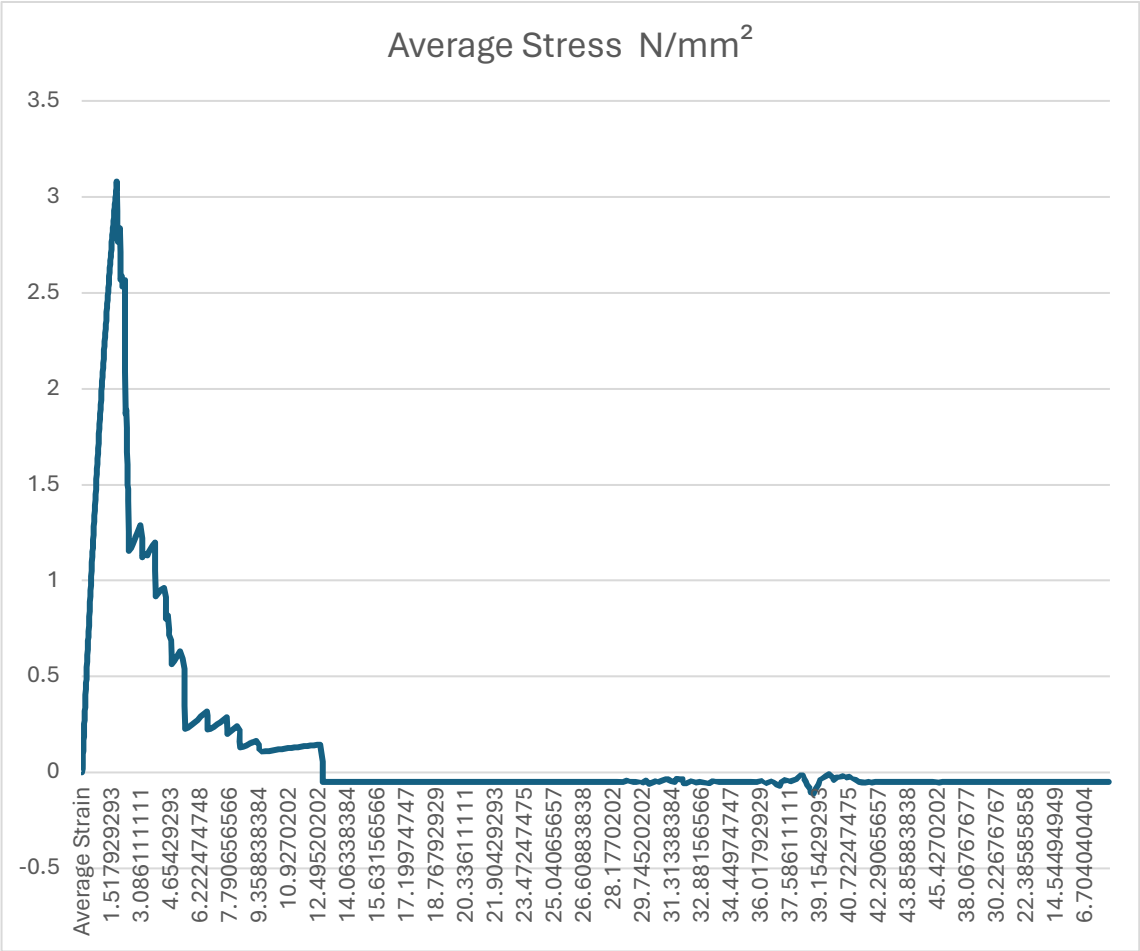

(ii) Translucent Resin

All geometries had multiple internal breakages before a final break. The simple grid design demonstrated the best tensile property by having a peak stress value of 1.337 N/mm^2 whilst the geometry with the least tensile strength was the grid with diamond hole a stress value of 1.048 N/mm^2. Below are the plots for the various geometries. Offset grid was not printed due challenges encountered during print with this specific resin.

Figure 3.2. 4 Stress-strain plot: Simple grid

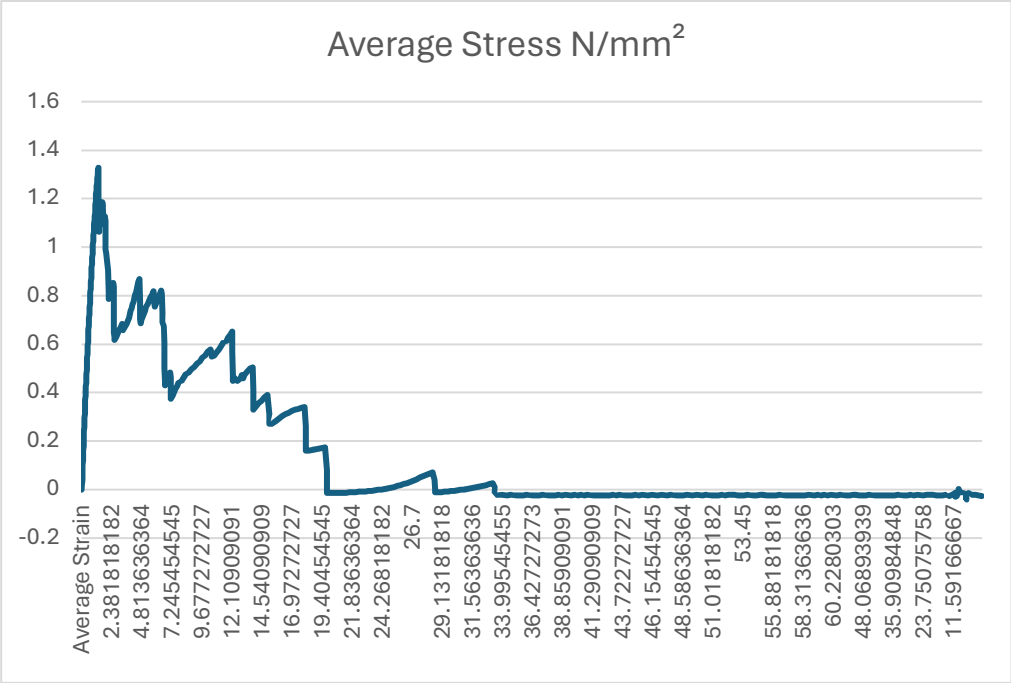

Figure 3.2. 5 Stress-strain plot: Grid with diamond holes

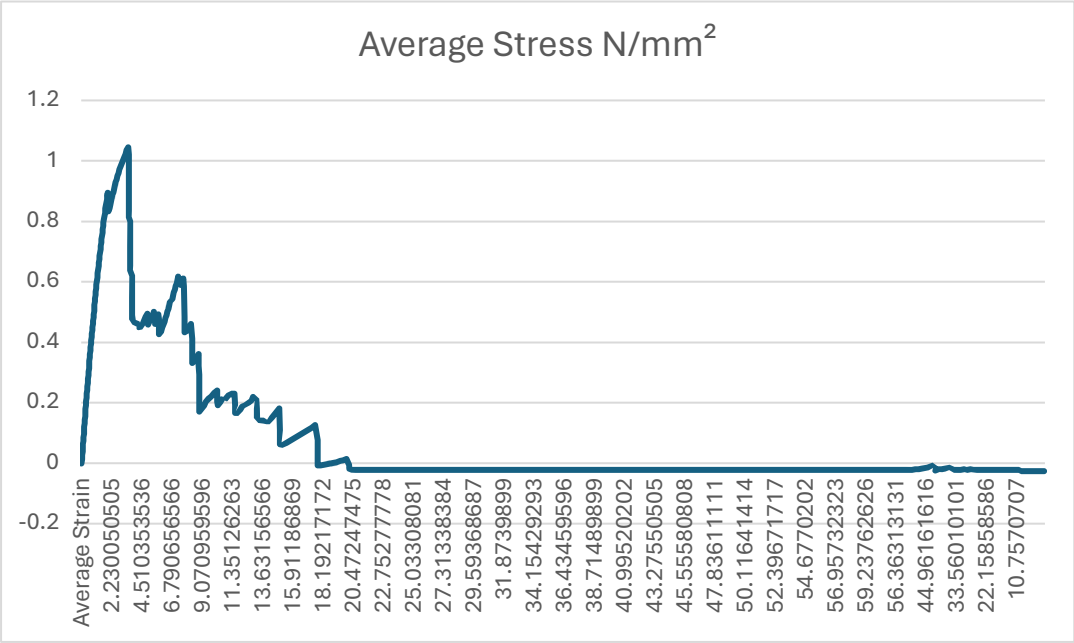

(iii) Water-Washable Resin

The simple grid design demonstrated the best tensile property by having a peak stress value of 2.653 N/mm^2 whilst the geometry with the least tensile strength was the offset grid with a stress value of 0.682N/mm^2. Grid with diamond holes had an ultimate tensile strength value of 1.641 N/mm^2

Figure 3.2. 6 Stress-strain plot: Simple grid.

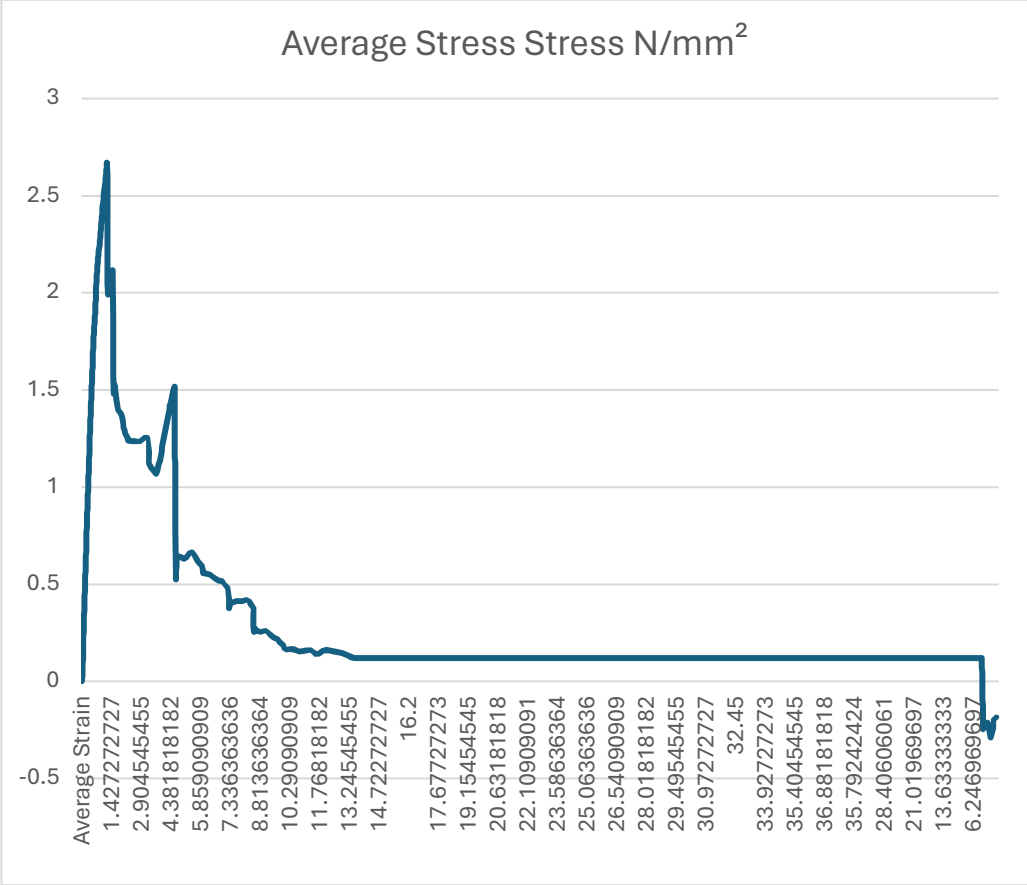

Figure 3.2. 7 Stress-strain plot: Offset Simple grid.

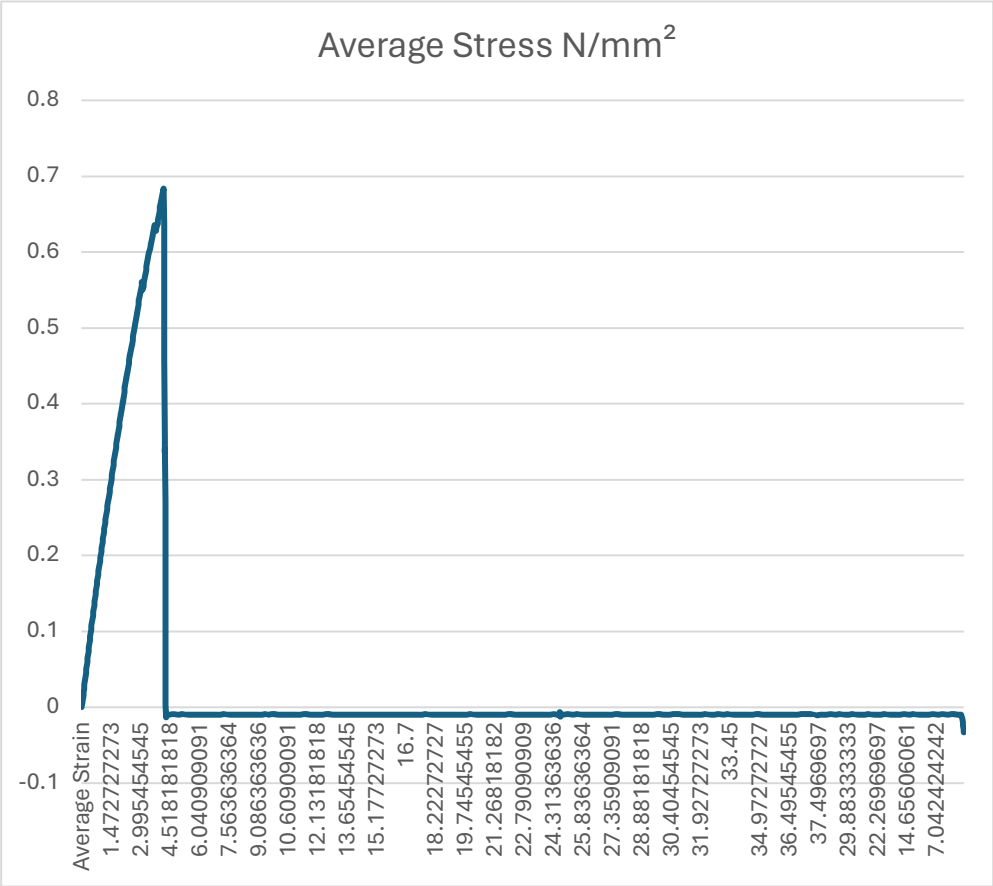

Figure 3.2. 8 Stress-strain plot: Grid with diamond holes.

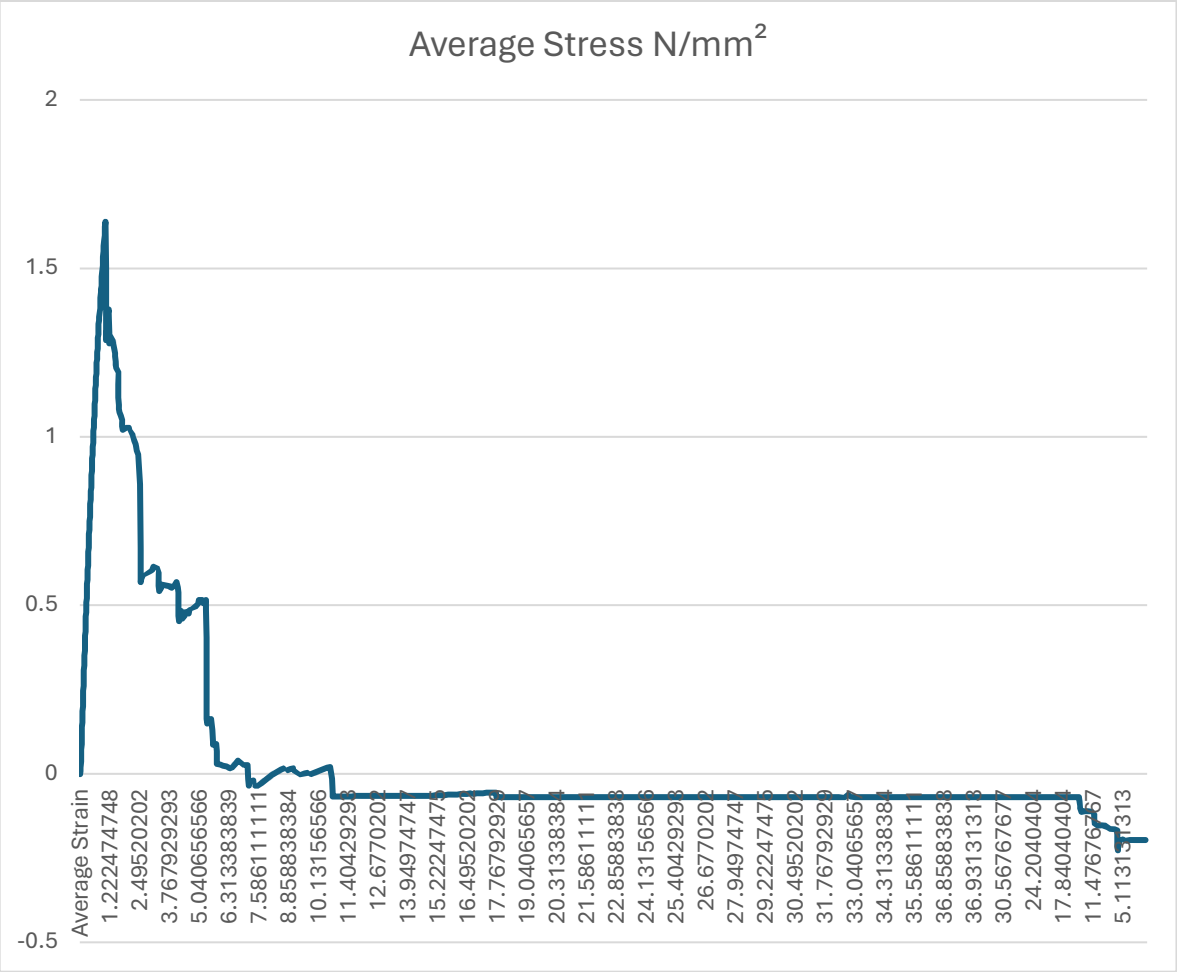

(iv) ABS-like Resin

The simple grid design demonstrated the best tensile property by having a peak stress value of 2.848 N/mm^2 whilst the geometry with the least tensile strength was the grid with diamond hole with a stress value of 1.842 N/mm^2. Diamond with holes exhibited a slight yield point. Below are the plots for the various geometries. Offset grid was not printed due challenges encountered during printing with this specific resin.

Figure 3.2. 9 Simple grid

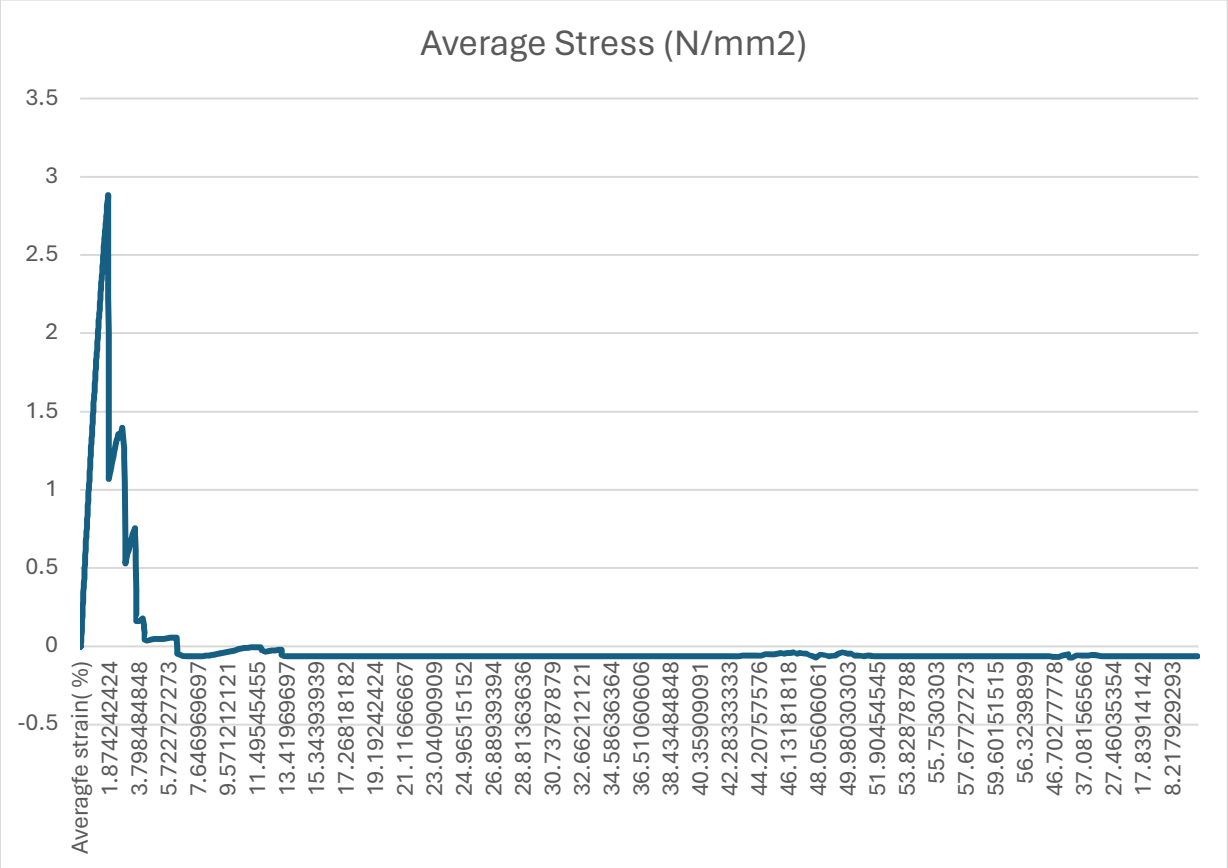

Figure 3.2. 10 Grid with diamonds

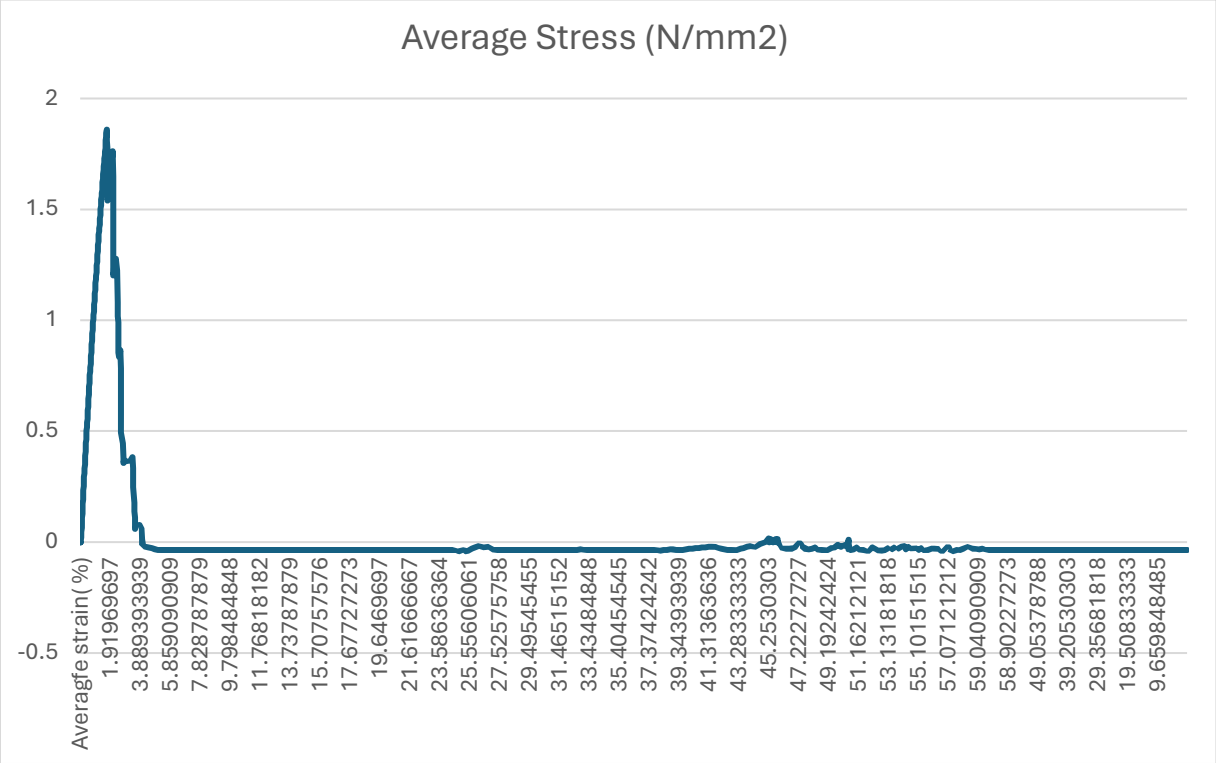

(v) Thermochromic Resin

The simple grid design demonstrated the best tensile property by having an ultimate tensile strength value of 4.148 N/mm^2 whilst the geometry with the least ultimate tensile strength was the offset grid with a stress value of 0.217 N/mm^2. Grid with diamond holes had an ultimate tensile strength value of 3.032 N/mm^2.

Figure 3.2. 11 simple grid

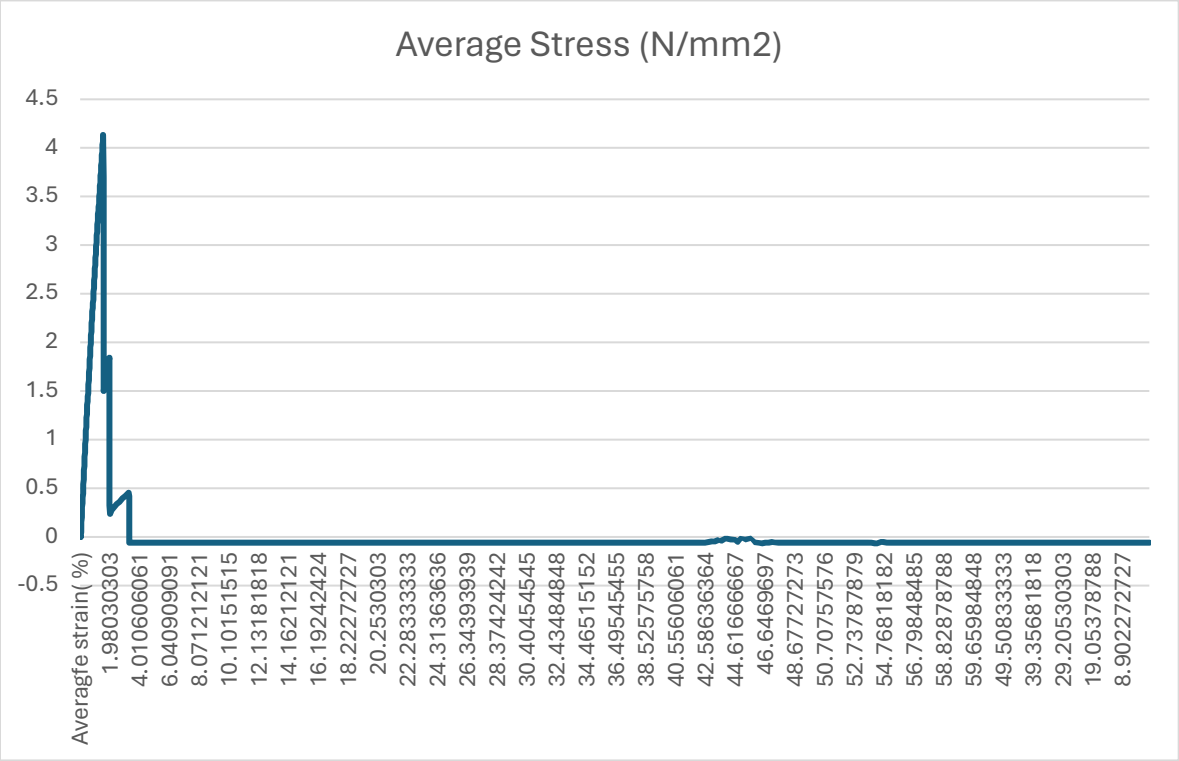

Figure 3.2. 12 Grid with diamond holes

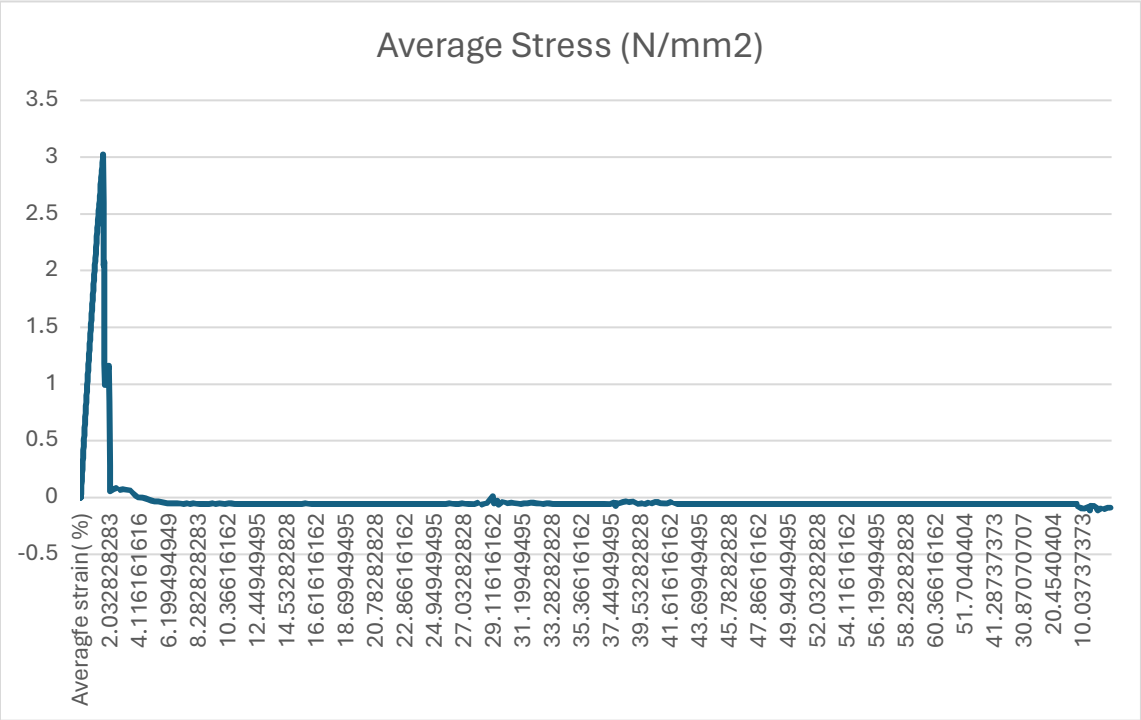

Figure 3.2. 13 Offset grid.

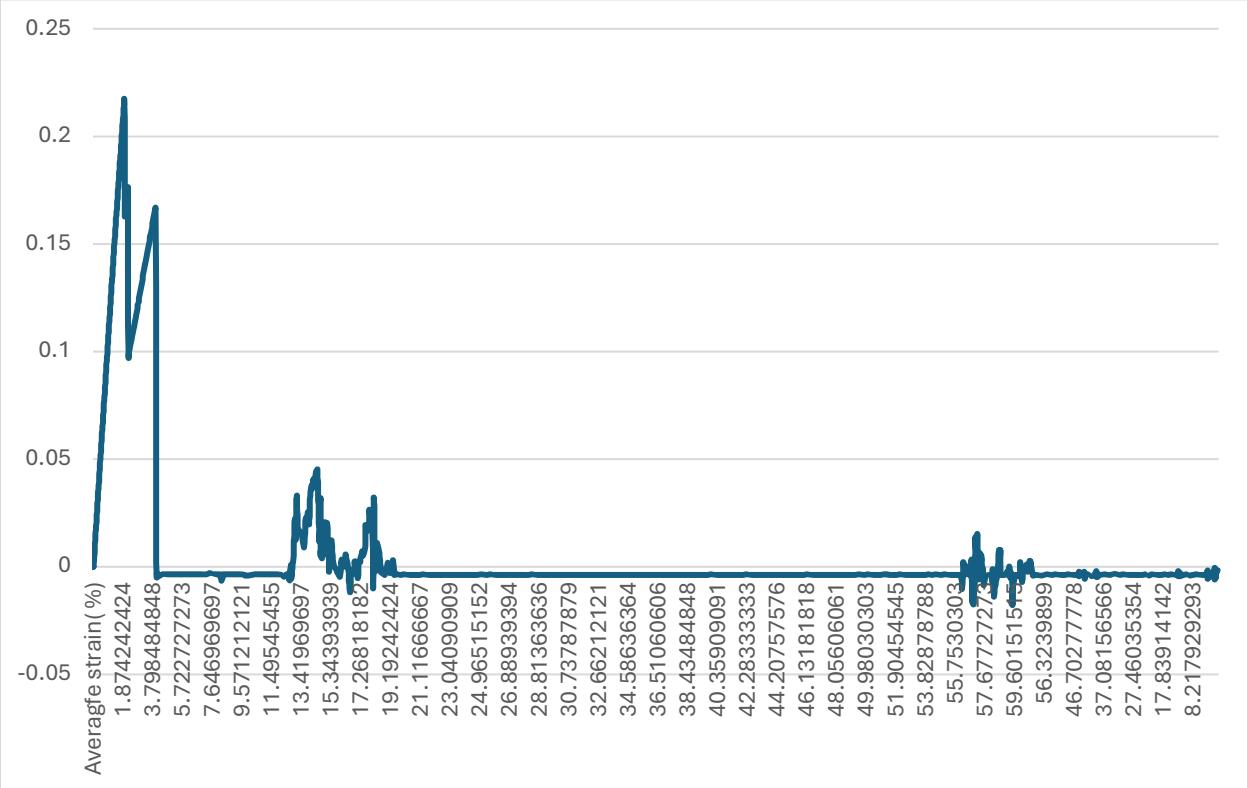

3.4. Young's modulus

The Young's modulus of elasticity was deduced by calculating the slope from the rising linear phase of the curves and the results represented in the table below.

Table 3. 2 indicating the deduction of young's modulus for various materials.

	YOUNG'S MODULUS(MPa)				
GEOMETRY	ABS-Like	Thermochromic resin	Standard Plant Photopolymer	Translucent Resin	Water-Washable
Simple Grid	1.141884	2.699259	2.298995	1.083183	2.221889
Offset simple grid		0.1110142	0.24774		0.168023
Grid with diamond holes	0.525192	1.932412	1.675186	0.44335	1.61236

With a P-Value of 0.05, a T-test = T-TEST=0.000829 indicates a significant difference among the Young's modulus value for simple grid and grid with diamonds.

Figure 3.2. 14 a bar chart indicating Young's Modulus values against various resins designs.

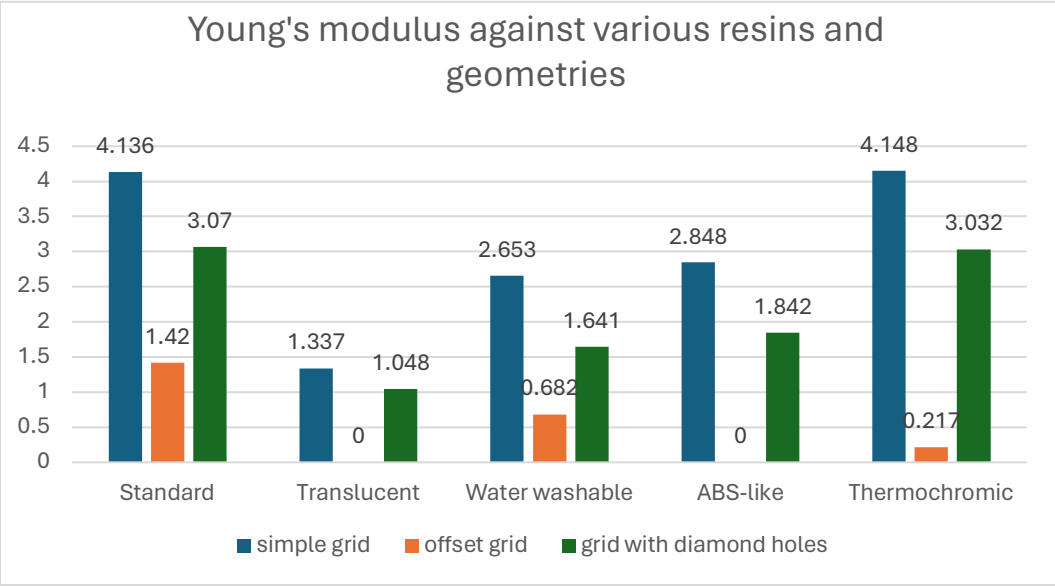

CHAPTER IV: DISCUSSION

The mechanical properties of various geometries and resin types were analyzed, focusing on the effect of geometric designs, the impact of resin type on mechanical performance, and challenges encountered during printing. Key mechanical properties, such as ultimate tensile strength (UTS), Young's modulus, break strain, and elastic behavior, were examined to assess the structural integrity, stiffness, ductility, and deformation characteristics of the printed prototypes.

4.1 Impact of Geometric Designs and Resin Types on Mechanical Properties.

The ultimate tensile strength values for (standard photopolymer resin) were 4.136 N/mm² for the simple grid geometry, 1.42 N/mm² for the offset grid, and 3.07 N/mm² for the grid with diamond holes. The Young's modulus values were 2.298995 MPa for the simple grid, 0.24774 MPa for the offset grid, and 1.675186 MPa for the grid with diamond holes. Also, the break strain values were 12.81% for the simple grid, 10.00% for the offset grid, and 13.00% for the grid with diamond holes as shown in figure 3.2.1- figure 3.2.3. The offset grid exhibited slight elastic behavior, indicating some flexibility.

As indicated in figure 3.2.4 and figure 3.2.5, the ultimate tensile strength values for (translucent resin) were 1.337 N/mm² for the simple grid geometry and 1.048 N/mm² for the grid with diamond holes. Unfortunately, the offset grid was not printed due to constant adhesion to the print platform, leading to breakage during removal. Similarly, the Young's modulus values were 1.083183 MPa for the simple grid and 0.44335 MPa for the grid with diamond holes, as the offset grid was not printed due to printing challenges with this resin. The break strain values were 20.10% for the simple grid and 20.35% for the grid with diamond holes. There was not a significant elastic region observed among these two geometries.

From figure 3.2.6- figure 3.2.8, the ultimate tensile strength values for (water washable photopolymer resin) were 2.653 N/mm² for the simple grid geometry, 0.682 N/mm² for the offset grid, and 1.641 N/mm² for the grid with diamond holes. The Young's modulus values were 2.221 MPa for the simple grid, 0.168 MPa for the offset grid, and 1.612 MPa for the grid with diamond holes. The break strain values were 6.246% for the simple grid, 4.442% for the offset grid, and 10.608% for the grid with diamond holes. The offset grid exhibited a slight elastic region.

The ultimate tensile strength values for (ABS-like resin) were 2.848 N/mm² for the simple grid geometry and 1.842 N/mm² for the grid with diamond holes. Unfortunately, the offset grid was not printed due to constant adhesion to the print platform, leading to breakage during removal. The Young's modulus values were 1.141 MPa for the simple grid and 0.525 MPa for the grid with diamond holes, as the offset grid was not printed due to printing challenges with this resin. Additionally, the break strain values were 4.586% for the simple grid, and 4.412% for the grid with diamond holes. The grid with diamond holes exhibited a slight yield point as depicted in figure 3.2.9 and figure 3.2.10.

As shown in figure 3.2.11- figure 3.2.13, the ultimate tensile strength values for thermochromic resin were 4.148 N/mm² for the simple grid geometry, 0.217 N/mm² for the offset grid, and 3.032 N/mm² for the grid with diamond holes. The Young's modulus values for this same resin were 2.699 MPa for the simple grid, 0.111 MPa for the offset grid, and 1.932 MPa for the grid with diamond holes. The break strain values were 3.518% for the simple grid, 4.192% for the offset grid, and 3.691% for the grid with diamond holes. The offset grid exhibited slight elastic behavior.

The UTS values across different geometric designs and resin types reveal significant variations in mechanical strength. The simple grid geometry exhibited the highest UTS values

for most resin types, with values ranging from 1.337 N/mm² to 4.148 N/mm² across different resin types exhibiting its ability to withstand maximum stress before breakage. On the other hand, the offset grid design consistently demonstrated the lowest UTS values, ranging from 0.217 N/mm² to 1.42 N/mm², indicating limitations in tensile strength. The simple grid geometry consistently demonstrated higher Young's modulus values, ranging from 1.083 MPa to 2.699 MPa indicating greater stiffness and potential for providing structural rigidity in knee brace applications.

Break strain values offer insights into the ductility and deformation characteristics of the materials. The grid with diamond holes designs generally exhibited higher break strain values, ranging from 3.032% to 20.35%, indicating better ductility and ability to undergo deformation before failure.

Finding the ideal material for knee brace customization is indeed a complex task due to various factors like comfort, strength, flexibility, and compatibility. Each material possesses its own set of advantages and disadvantages, and it's essential to weigh these factors carefully to make an informed decision. A study by Mian et al. reinforces this observation, highlighting that no single material possesses all the desired benefits. In their examination of the mechanical, physical, and dimensional characteristics of 3D printing materials such as PLA, ABS, PETG, TPU, and PP, they concluded that each material has its own strengths and weaknesses (Mian et al., 2024) hence using materials to their strength could be beneficial.

4.2 Challenges Encountered.

There were printing challenges associated with the offset grid design using translucent and ABS-like resin types. Constant adhesion to the print platform resulted in breakages during removal, indicating difficulties in achieving successful prints with this geometry and resin

combination. The observation of a slight elastic region in the offset grid design suggests flexibility and potential for dynamic support during movement.

CHAPTER V: CONCLUSION AND FUTURE DIRECTION

Choosing the appropriate material for a component is critical. It is necessary to thoroughly assess all available materials before deciding, ensuring compatibility with the intended application. Optimization efforts should focus on balancing mechanical strength, stiffness, and ductility to meet the diverse requirements of knee brace applications.

In conclusion, the simple grid geometry consistently demonstrated higher UTS values, highlighting its superior ability to withstand maximum stress before breakage. Contrary, the offset grid design consistently showed lower UTS values, indicating limitations in tensile strength. Also, the simple grid geometry consistently exhibited higher Young's modulus values, suggesting greater structural rigidity and potential for providing robust support in knee brace applications.

The grid with diamond holes exhibited the best mechanical properties that might be suitable for future knee brace customization. The grid with diamond holes designs generally displayed higher break strain values, indicating better ductility and resistance to deformation before failure. This also indicates its ability to undergo multiple internal breakages before fracture. Thermochromics and standard photopolymer resin exhibited the highest ultimate tensile strength.

Despite these promising findings, challenges were encountered, particularly with the offset grid design using certain resin types. It is observed that every material has advantages and disadvantages and hence no single material is particularly suitable for knee brace customization taking into consideration factors such comfort, strength, flexibility, and compatibility. Printing difficulties, such as constant adhesion to the print platform, resulted in breakages during removal, highlighting the need for further optimization in additive manufacturing processes. The

findings of this study contribute to advancing knowledge in additive manufacturing for knee brace design.

5.1 Future research directions

By understanding the relationship between geometric design, material properties, and printing challenges, future research endeavors can focus on

- Investigating alternative 3D printing methods and their potential effects on mechanical properties.
- Exploring a variety of designs and fine-tuning design parameters for optimization.
- Considering additional mechanical properties, such as compression, to provide further analysis.
- There could also be a possibility in combining different designs and materials for a diverse outcome.
- Explore the inclusion of nanoparticles could also be an area of investigation.

REFERENCES.

Ahangar, P., Cooke, M. E., Weber, M. H., & Rosenzweig, D. H. (2019). Current biomedical applications of 3D printing and additive manufacturing. In Applied Sciences (Switzerland) (Vol. 9, Issue 8). https://doi.org/10.3390/app9081713

Chohan, J. S., Singh, R., Boparai, K. S., Penna, R., & Fraternali, F. (2017). Dimensional accuracy analysis of coupled fused deposition modeling and vapour smoothing operations for biomedical applications. Composites Part B: Engineering, 117, 138–149. https://doi.org/10.1016/j.compositesb.2017.02.045

Dou, R., Wang, T., Guo, Y., & Derby, B. (2011). Ink-Jet Printing of Zirconia: Coffee Staining and Line Stability. Journal of the American Ceramic Society, 94(11), 3787–3792. https://doi.org/10.1111/j.1551-2916.2011.04697.x

Gibson, I., Rosen, D., & Stucker, B. (2015). Sheet Lamination Processes. In Additive Manufacturing Technologies (pp. 219–244). Springer New York. https://doi.org/10.1007/978-1-4939-2113-3_9

Gioumouxouzis, C. I., Karavasili, C., & Fatouros, D. G. (2019). Recent advances in pharmaceutical dosage forms and devices using additive manufacturing technologies. Drug Discovery Today, 24(2), 636–643. https://doi.org/10.1016/j.drudis.2018.11.019

Haglin, J. M. ; E. A. E. ; G. J. A. ; M. S. E. ; B.-H. J. ; D. A. H. (2016). Patient-Specific Orthopaedic Implants. Pubmed, 417–424.

Hahnlen, R., & Dapino, M. J. (2014). NiTi–Al interface strength in ultrasonic additive manufacturing composites. Composites Part B: Engineering, 59, 101–108. https://doi.org/10.1016/j.compositesb.2013.10.024

Khoshnevis, B. (2004). Automated construction by contour crafting - Related robotics and information technologies. Automation in Construction, 13(1), 5–19. https://doi.org/10.1016/j.autcon.2003.08.012

Labeaga-Martínez, N., Sanjurjo-Rivo, M., Díaz-Álvarez, J., & Martínez-Frías, J. (2017). Additive manufacturing for a Moon village. Procedia Manufacturing, 13, 794–801. https://doi.org/10.1016/j.promfg.2017.09.186

Lakkala, P., Munnangi, S. R., Bandari, S., & Repka, M. (2023). Additive manufacturing technologies with emphasis on stereolithography 3D printing in pharmaceutical and medical applications: A review. International Journal of Pharmaceutics: X, 5. https://doi.org/10.1016/j.ijpx.2023.100159

Li, J., Wu, C., Chu, P. K., & Gelinsky, M. (2020). 3D printing of hydrogels: Rational design strategies and emerging biomedical applications. In Materials Science and Engineering R: Reports (Vol. 140). Elsevier Ltd. https://doi.org/10.1016/j.mser.2020.100543

Ngo, T. D., Kashani, A., Imbalzano, G., Nguyen, K. T. Q., & Hui, D. (2018). Additive manufacturing (3D printing): A review of materials, methods, applications and challenges. In Composites Part B: Engineering (Vol. 143, pp. 172–196). Elsevier Ltd. https://doi.org/10.1016/j.compositesb.2018.02.012

Pattinson, S. W., Huber, M. E., Kim, S., Lee, J., Grunsfeld, S., Roberts, R., Dreifus, G., Meier, C., Liu, L., Hogan, N., & Hart, A. J. (2019). Additive Manufacturing of Biomechanically Tailored Meshes for Compliant Wearable and Implantable Devices. Advanced Functional Materials, 29(32). https://doi.org/10.1002/adfm.201901815

Pere, C. P. P., Economidou, S. N., Lall, G., Ziraud, C., Boateng, J. S., Alexander, B. D., Lamprou, D. A., & Douroumis, D. (2018). 3D printed microneedles for insulin skin delivery.

International Journal of Pharmaceutics, 544(2), 425–432. https://doi.org/10.1016/j.ijpharm.2018.03.031

Rengier, F., Mehndiratta, A., Von Tengg-Kobligk, H., Zechmann, C. M., Unterhinninghofen, R., Kauczor, H. U., & Giesel, F. L. (2010). 3D printing based on imaging data: Review of medical applications. In International Journal of Computer Assisted Radiology and Surgery (Vol. 5, Issue 4, pp. 335–341). Springer Verlag. https://doi.org/10.1007/s11548-010-0476-x

Stansbury, J. W., & Idacavage, M. J. (2016). 3D printing with polymers: Challenges among expanding options and opportunities. Dental Materials, 32(1), 54–64. https://doi.org/10.1016/j.dental.2015.09.018

Travitzky, N., Bonet, A., Dermeik, B., Fey, T., Filbert-Demut, I., Schlier, L., Schlordt, T., & Greil, P. (2014). Additive Manufacturing of Ceramic-Based Materials. Advanced Engineering Materials, 16(6), 729–754. https://doi.org/10.1002/adem.201400097

Wang, X., Jiang, M., Zhou, Z., Gou, J., & Hui, D. (2017). 3D printing of polymer matrix composites: A review and prospective. Composites Part B: Engineering, 110, 442–458. https://doi.org/10.1016/j.compositesb.2016.11.034

Wu, P., Wang, J., & Wang, X. (2016). A critical review of the use of 3-D printing in the construction industry. Automation in Construction, 68, 21–31. https://doi.org/10.1016/j.autcon.2016.04.005

Zadpoor, A. (2017). Design for Additive Bio-Manufacturing: From Patient-Specific Medical Devices to Rationally Designed Meta-Biomaterials. International Journal of Molecular Sciences, 18(8), 1607. https://doi.org/10.3390/ijms18081607

Mian, S. H., Abouel Nasr, E., Moiduddin, K., Saleh, M., & Alkhalefah, H. (2024). An Insight into the Characteristics of 3D Printed Polymer Materials for Orthoses Applications: Experimental Study. Polymers, 16(3). https://doi.org/10.3390/polym16030403